A&A 447, L9–L12 (2006)
DOI: 10.1051/0004-6361:200500230

Astronomy & Astrophysics

Evidence supporting the kinematic interpretation of water maser proper motions

C. Goddi[1], L. Moscadelli[1], J. M. Torrelles[2,⋆], L. Uscanga[3], and R. Cesaroni[4]

[1] INAF, Osservatorio Astronomico di Cagliari, Loc. Poggio dei Pini, Str. 54, 09012 Capoterra (CA), Italy
e-mail: cgoddi@ca.astro.it
[2] Instituto de Ciencias del Espacio (CSIC)–IEEC, Gran Capitá 2, 08034 Barcelona, Spain
[3] Instituto de Astronomía, UNAM, Apdo. Postal 70-264, 04510 México, D.F., México
[4] INAF, Osservatorio Astrofisico di Arcetri, Largo E. Fermi 5, 50125 Firenze, Italy

Received 7 December 2005 / Accepted 21 December 2005

ABSTRACT

We have analyzed multi-epoch 22 GHz water maser observations performed with the Very Long Baseline Array (VLBA) towards the high-mass star forming region (SFR) G24.78+0.08. The spatial structure of the water maser integrated intensity has been obtained at three different epochs and found to maintain a very remarkable persistent morphology over the three epochs. Evidence of systematic (expanding) motions for the whole structure traced by the maser emission is also reported. In addition, we have obtained, from previously reported data, the integrated emission of a cluster of water masers spread over $\simeq$ 10 mas within the expanding shell of $\simeq$0.16″ size around the young stellar object W75 N (B)-VLA 2. As in G24.78+0.8, we also find that the morphology of the integrated intensity of the water masers of this cluster persists over different observed epochs. These results strongly support the interpretation that the measured proper motions of the water masers are due to real physical motions of distinct blobs of maser-emitting gas, rather than to other effects, such as a travelling background illuminating wave or turbulence in the circumstellar medium. This result is crucial in astrophysical applications of maser proper-motion measurements, including distance determinations and studies of circumstellar gas kinematics in SFRs and late-type stars.

Key words. masers – stars: formation – ISM: kinematics and dynamics

1. Introduction

The environment of SFRs is looked for and studied by means of numerous tracers, such as the "free-free" emission of the ionized gas, the thermal continuum of the dust heated by the stellar radiation, and thermal lines of rotational transitions of many interstellar molecules. A few molecular transitions are observed to emit as masers, and particularly interesting for their elevated flux densities and ubiquity are the 22.2 GHz H_2O maser and the CH_3OH 6.7 GHz and 12 GHz masers. The use of maser emission to determine the physical conditions of the gas is made difficult owing to the fact that the maser lines originate in non-LTE conditions. However, since maser amplification requires high line-of-sight velocity coherence, maser emission can be valuable to study the kinematics of ordered velocity fields, such as those associated with jets/outflows, disks, and expanding/contracting shells. Very Long Baseline Interferometry (VLBI) observations have revealed that the maser emission originates from compact (<10 AU) and bright ($T_b > 10^9$ K) emission centres (maser spots), characterized by a well defined line-of-sight velocity. VLBI observations provide accurate positions and line-of-sight velocities of the maser spots, and, by comparing measurements over several epochs, proper motions of the maser spots can be derived. For the 22 GHz H_2O masers ($6_{16} \rightarrow 5_{23}$), the amplitude of observed proper motions varies typically in the interval ~0.1–1 mas/month, corresponding to linear velocities from tens to hundreds km s^{-1}, for a source at a distance of 1 kpc. Given the typical angular resolution achievable with the VLBI at 22 GHz (~0.5 mas), the proper motions of the water masers are measurable with time baselines as short as a few weeks/months. The measured tangential velocities, combined with the radial velocities derived via the Doppler effect, permit us to obtain the three-dimensional (3-D) velocity distribution of the masing gas.

The first multi-epoch VLBI observations of the water masers were performed about 20 years ago towards a few of the strongest 22 GHz H_2O sources in the Galaxy, i.e. Orion-KL (Genzel et al. 1981a), W51 (Genzel et al. 1981b), Sagittarius B2 N (Reid et al. 1988), W49 (Gwinn et al. 1992), and allowed both the determination of the characteristic pattern of the kinematics of these regions and, by comparing the line-of-sight velocities with the proper motions of the maser spots,

⋆ On sabbatical leave at the United Kingdom Astronomy Technology Centre, Royal Observatory Edinburgh, UK.

the derivation of accurate source distances. More recently, this technique has been successfully employed by several authors (Claussen et al. 1998; Furuya et al. 2000; Imai et al. 2000; Torrelles et al. 2001a,b, 2003; Furuya et al. 2005; Goddi et al. 2005; Goddi & Moscadelli 2005; Moscadelli et al. 2005) to study the kinematics of the circumstellar gas in a sample of SFRs. Such studies indicate that water masers are preferentially associated with well-collimated (jets) or wide-angle flows of gas at the base of larger-scale molecular outflows.

A basic assumption of multi-epoch VLBI studies is that the measured proper motions reflect real movements of maser-emitting gas. As the number of sources studied by means of H_2O maser VLBI observations increases, we feel the need to discuss more thoroughly this assumption.

Within this letter, we present an analysis of the multi-epoch VLBA observations of the 22 GHz H_2O masers carried out towards two SFRs, showing that the best interpretation of the spot proper motions is in terms of physical motions of the maser-emitting gas.

2. Data analysis

Water maser proper motion measurements towards the high-mass SFRs G24.78+0.08 and W75 N (B) have been recently obtained with the VLBA of the NRAO[1]. An extensive description of the observations and data reduction process will be and has been provided by Moscadelli et al. (in prep.) and Torrelles et al. (2003) for G24.78+0.08 and W75 N (B), respectively.

Figures 1 and 2 compare the 22 GHz maser spectra and integrated intensity structures obtained over the three observational epochs for specific subregions of the water maser shells found in G24.78+0.08 and around the compact radio continuum source W75 N (B)-VLA 2, respectively. The integrated intensity maps have been aligned at the position of the peak integrated intensity of the first epoch (feature "A" for both regions) for an easier visual structural comparison between epochs. The integrated intensity of the different water maser features varies among epochs by a factor of ∼2 and ∼6 for the specific subregions plotted in Figs. 1 and 2, respectively. Large intensity variations are commonly observed in water maser sources on short (days and weeks) and long (months and years) timescales (Brand et al. 2003) and may be explained by changes in the orientation of the maser beam and/or in the maser pump and velocity coherence (Elitzur et al. 1992). For both sources, it was possible to measure the relative positions of the maser features with an accuracy better than 0.3 mas. The measured amplitude of the proper motions (shown in Figs. 1 and 2) varies in the range ∼0.3–2.7 and 1.7–3.0 mas yr^{-1}, corresponding to linear velocities of ∼11–99 and 16–28 km s^{-1} for G24.78+0.08 (at a distance of 7.7 kpc) and W75 N (at a distance of 2 kpc), respectively.

[1] The National Radio Astronomy Observatory is a facility of the National Science Foundation operated under cooperative agreement by Associated Universities, Inc.

3. Discussion

Bloemhof et al. (1996) measured intrinsic morphologies of OH masers towards the UC HII region W3(OH). In particular, they fitted elliptical Gaussians to the maser features and compared the orientations of corresponding maser features at different observational epochs as measured by the position angle of the Gaussian fit. The shapes and orientations of OH masers are found to remain remarkably persistent in time, suggesting that the measured proper motions are due to actual physical motion of individual clumps of maser-emitting gas. Unlike OH masers, H_2O maser features are in general spatially unresolved. Even if for the H_2O masers it is not possible to prove the time persistence basing on individual spot morphologies, one can consider the overall structure of the maser emission. Although the intensity of the different maser spots varies from epoch to epoch, visual inspection of both the spectra and the maps of G24.78+0.08 and W75 N (B) at the three epochs clearly shows that the *whole* spatial-velocity structure of maser emission persists in time (over a few months). In particular, in each of the observing epochs, maser emission shows approximately the same number of intensity peaks with the same (within a few tenths of milliarcseconds) relative spatial displacements. In both sources, the measured proper motions clearly indicate ordered (expanding) motions of the whole structure of the masing gas (Moscadelli et al., in prep.; Torrelles et al. 2003).

In the following, we discuss plausible physical processes, alternative to real motions of maser-emitting gas, which might account for the maser features' proper motions observed in these two sources: 1) an excitation radiative front; 2) a moving background source of radiation; 3) a random variation of coherent velocity paths.

The first mechanism assumes that an excitation radiative front heats the dust grains inducing desorption of H_2 molecules, which in turn would excite the H_2O masers by collisions. As long as the excitation front propagates across the circumstellar gas, different portions of gas would be excited, resulting in apparent motions of the masing gas (Deguchi 1982). However, since such front would move with a velocity very close to the speed of light, the proper motions measured towards G24.78+0.08 and W75 N (B) are several orders of magnitude too low to be explained with such a mechanism.

In principle, also a source (e.g., a shock wave) travelling behind an inverted layer of stationary gas might result in apparent motions of the masing gas (Deguchi 1982). The intensity of maser radiation depends essentially upon the background radiative field, the pumping efficiency, the amplification path (the column density of inverted masing molecules with the same line of sight velocity), and the maser geometry. In both G24.78+0.08 and W75 N (B), the maser emission arises from regions of sizes from tens to hundreds of AU, across which the background radiative field and the pumping conditions can be expected to be substantially constant, so that the variation of maser intensity should be due to changes in the column density of inverted (velocity coherent) masing molecules of the stationary layer of gas. Along the arc-like profile traced by H_2O masers in G24.78+0.08 the emission concentrates in compact spots and changes abruptly its morphology on length scales of a

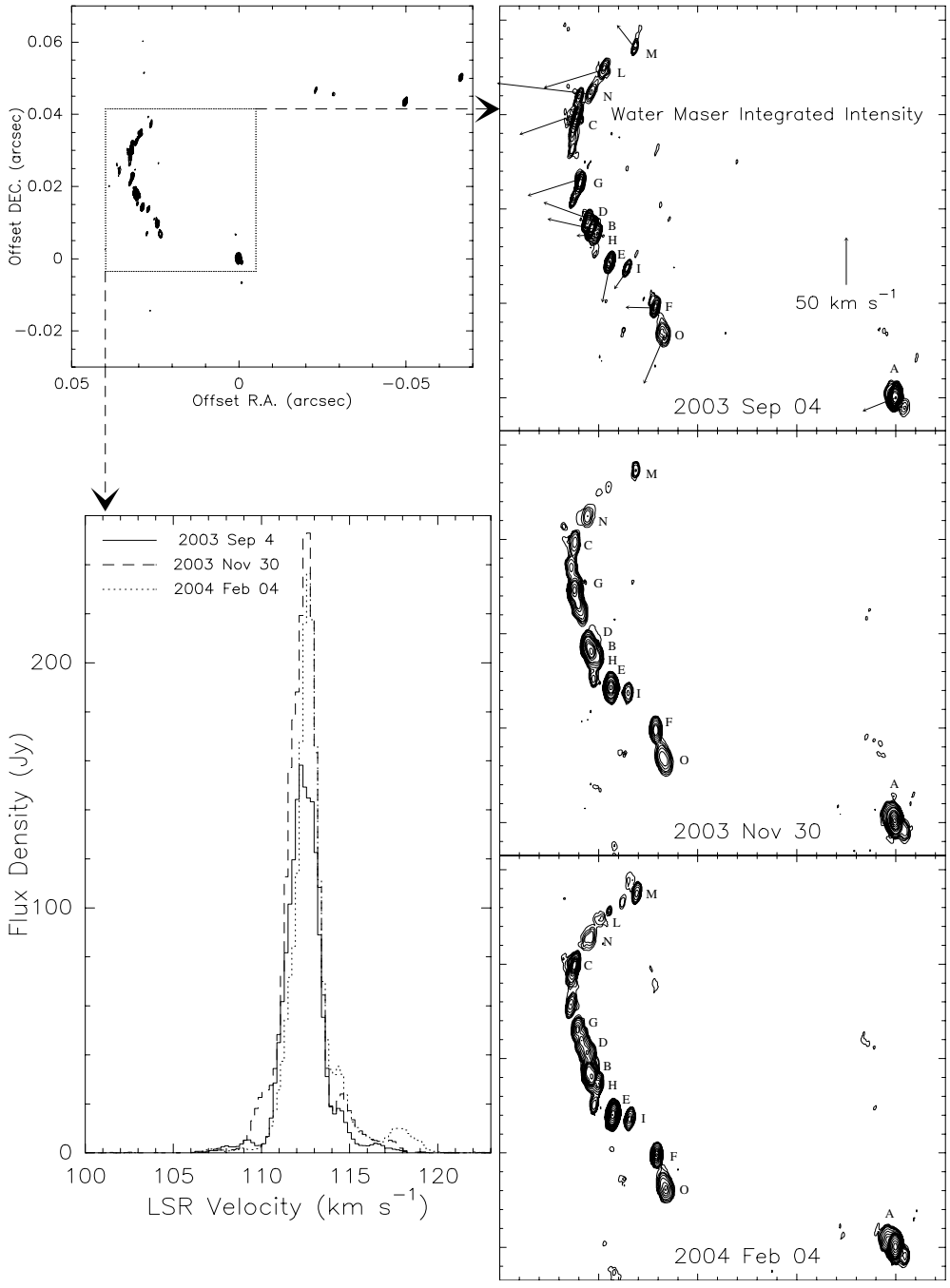

Fig. 1. (*Upper left-hand panel*) Positions of the water masers of the expanding shell found in G24.78+0.08. (*Bottom left-hand panel*) Integrated flux density spectra of the region of the shell indicated by a square. (*Right-hand panels*) Comparison of the structure of the integrated H_2O maser emission between three VLBA observational epochs. In each panel, the maser emission has been integrated over the velocity interval 106.8–118.4 km s^{-1}. Contour levels (selected to distinguish the different peaks of the emission) are: 100 mJy beam^{-1} km s^{-1} × (1, 3, 6, 10, 20, 30, 50, 70, 100, 150, 200, 300, 400, 600), 100 mJy beam^{-1} km s^{-1} × (1, 3, 6, 10, 20, 40, 70, 100, 200, 300, 400, 600, 800, 1000), and 60 mJy beam^{-1} km s^{-1} × (1, 3, 6, 10, 20, 40, 70, 100, 130, 160, 200, 300, 500, 800, 1100, 1450) for the first, second, and third observed epoch, respectively. The different masers persisting in the three epochs and where it was possible to measure proper motions are labelled with capital letters, following a decreasing order of intensity as observed in the first epoch. The maps have been aligned at the position of the strongest feature detected in the first epoch with label letter "A" for an easier comparison between epochs. The arrows indicate the measured proper motions, whose amplitude scale is given in the right-hand side of the panel.

few AU. On such scales, the properties of this layer of gas may be expected to be the same both *along* and *across* the arc-like profile of maser emission. Hence, as long as the background source propagates and is amplified by the foreground masing gas, time variations of maser spot intensity of the same order as observed at a given epoch along the arc-like profile, should be observed. Figure 1 shows, however, that the integrated intensity structure of the maser emission persists over the three

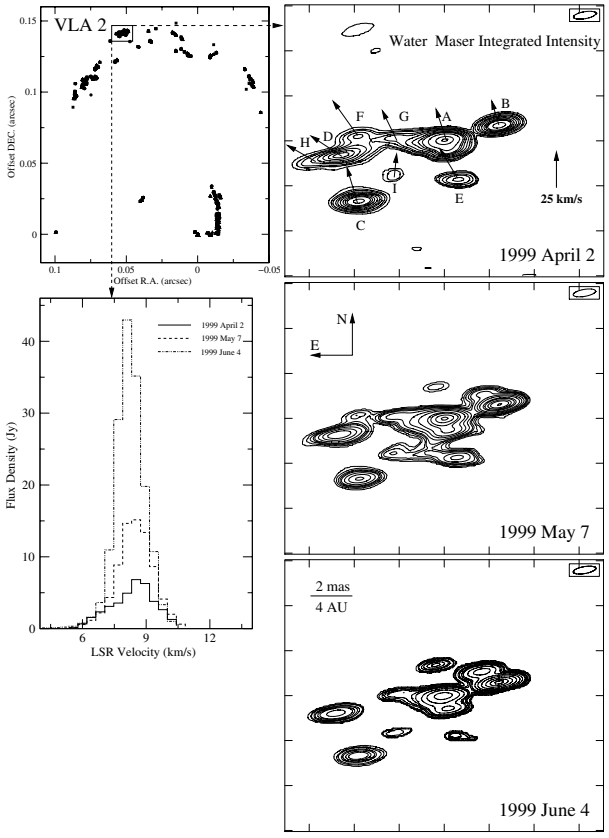

Fig. 2. (*Upper left-hand panel*) Positions of the water masers of the expanding shell around the compact radio continuum source W75 N(B)-VLA2 (from Torrelles et al. 2003). (*Bottom left-hand panel*) Integrated flux density spectra of the region of the VLA 2 shell indicated by a square. (*Right-hand panels*) Comparison of the structure of the integrated H_2O maser emission between three VLBA observational epochs. In each panel, the maser emission has been integrated over the velocity interval 4.5–11 km s^{-1}. Contour levels are: 30 mJy km s^{-1} × (1, 3, 5, 9, 13, 20, 30, 40, 50, 80, 150, 200), 20 mJy km s^{-1} × (3, 7, 11, 15, 19, 30, 50, 80, 150, 200, 300, 400, 600), and 25 mJy km s^{-1} × (1, 4, 7, 15, 20, 30, 40, 80, 150, 300, 600, 1000, 1400) for the first, second, and third observed epoch, respectively. As in Fig. 1, the maps have been aligned at the position of the feature with label letter "A", whereas the arrows indicate the proper motions measured by Torrelles et al. (2003).

epochs, which leads to rule out the moving background source as responsible for the measured proper motions.

In the third scenario maser features might be associated to randomly fluctuating velocity coherent paths in a turbulent medium, as first proposed by Deguchi (1982). This model predicts a random time variation of the higher amplification paths along the line of sight ("Christmas tree effect"), which may result in apparent proper motions of masing gas. Previous VLBI studies of proper motions of H_2O masers associated with YSOs (Gwinn 1994; Strelnitski et al. 2002; Imai et al. 2002) have revealed the presence of both an ordered (expanding and rotating) and a residual random (turbulent) components of motion. These works suggest that H_2O masers might trace a turbulent velocity field, with typical amplitudes of a few tens of km s^{-1}, over linear scales from 0.1 to 300 AU. Strelnitski et al. (2002) suggested a new conceptual model of excitation of H_2O masers, which proposes the maser pump to be the dissipation of turbulent energy produced by protostellar winds or jets (and not directly the mechanical energy carried by the wind/jet). Even if a certain degree of turbulence might be present in the water maser birthplaces, these previous observations have revealed that a systematic motion generally dominates. In any case, a "pure" turbulent medium would lead to a random pattern of maser motions, in disagreement with the observations of organized motions, such as those measured by us towards G24.78+0.08 and W75 N(B), and by other authors towards Sgr B2 N, W49 N, W3(OH), and W3 IRS 5.

In summary, the analysis of the data presented in this Letter lend support to the picture of water maser features as marking discrete clumps of moving gas and, hence, strongly support the validity of using water masers as kinematic probes.

References

Bloemhof, E. E., Moran, J. M., & Reid, M. J. 1996, ApJ, 467, L117
Brand, J., Cesaroni, R., Comoretto, G., et al. 2003, A&A, 407, 573
Claussen, M. J., Marvel, K. B., Wootten, A., & Wilking, B. A. 1998, ApJ, 507, L79
Deguchi, S. 1982, ApJ, 259, 634
Elitzur, M., Hollenbach, D. J., & McKee, C. F. 1992, ApJ, 394, 221
Furuya, R. S., Kitamura, Y., Wootten, A., Claussen, M. J., & Kawabe, R. 2005, A&A, 438, 571
Furuya, R. S., Kitamura, Y., Wootten, H. A., et al. 2000, ApJ, 542, L135
Genzel, R., Downes, D., Schneps, M. H., et al. 1981b, ApJ, 247, 1039
Genzel, R., Reid, M. J., Moran, J. M., & Downes, D. 1981a, ApJ, 244, 884
Goddi, C. & Moscadelli, L. 2005, ArXiv Astrophysics e-prints
Goddi, C., Moscadelli, L., Alef, W., et al. 2005, A&A, 432, 161
Gwinn, C. R. 1994, ApJ, 429, 241
Gwinn, C. R., Moran, J. M., & Reid, M. J. 1992, ApJ, 393, 149
Imai, H., Deguchi, S., & Sasao, T. 2002, ApJ, 567, 971
Imai, H., Kameya, O., Sasao, T., et al. 2000, ApJ, 538, 751
Moscadelli, L., Cesaroni, R., & Rioja, M. J. 2005, A&A, 438, 889
Reid, M. J., Schneps, M. H., Moran, J. M., et al. 1988, ApJ, 330, 809
Strelnitski, V., Alexander, J., Gezari, S., et al. 2002, ApJ, 581, 1180
Torrelles, J. M., Patel, N. A., Gómez, J. F., et al. 2001a, Nature, 411, 277
Torrelles, J. M., Patel, N. A., Gómez, J. F., et al. 2001b, ApJ, 560, 853
Torrelles, J. M., Patel, N. A., Anglada, G., et al. 2003, ApJ, 598, L115